Carbohydrate Polymers 96 (2013) 621–627

Contents lists available at SciVerse ScienceDirect

Carbohydrate Polymers

journal homepage: www.elsevier.com/locate/carbpol

Poly(lactic acid)/natural rubber/cellulose nanocrystal bionanocomposites. Part II: Properties evaluation

Natacha Bitinis[a], Elena Fortunati[b], Raquel Verdejo[a], Julien Bras[c], Jose Maria Kenny[a,b], Luigi Torre[b], Miguel Angel López-Manchado[a,*]

[a] Institute of Polymer Science and Technology, ICTP-CSIC, C/ Juan de la Cierva, 3, 28006 Madrid, Spain
[b] University of Perugia, UdR INSTM, Department of Civil and Environmental Engineering, I-05100 Terni, Italy
[c] Laboratory of Pulp and Paper Science, LGP2, F-38402 St Martin Dheres, France

ARTICLE INFO

Article history:
Received 18 December 2012
Received in revised form 14 February 2013
Accepted 20 March 2013
Available online 6 April 2013

Keywords:
Cellulose nanocrystal
Bionanocomposite
Poly(lactic acid)
Crystallization
Mechanical properties
Biodegradation

ABSTRACT

The crystallization, mechanical and biodegradation properties of poly(lactic acid)/natural rubber/cellulose nanocrystals (CNC) bionanocomposites were evaluated. Three types of CNC were used in this study, one unmodified (CNC), long alkyl chain grafted CNC (C18-g-CNC) and PLA grafted CNC (PLA-g-CNC). The CNC modifications determined the affinity of the nanocrystals toward the polymers and reflected on the ultimate properties. Interestingly, PLA-g-CNC acted as a nucleating agent for the PLA matrix in the bio-based PLA/NR blend. Good mechanical properties were reported, as the bionanocomposites maintained a high elongation at break for a concentration up to 3 wt.% of cellulose nanocrystals. Moreover, the disintegration study confirmed that the materials completely disintegrated after one month in compost.

1. Introduction

Cellulose is one of most abundant carbohydrate polymer produced by biomass, from which high modulus nanocrystals (CNC) can be extracted (Azizi Samir, Alloin, & Dufresne, 2005; Habibi, Lucia, & Rojas, 2010). These nanosized particles present the advantage of being renewable when compared to other inorganic fillers, which is of great interest regarding the reinforcement of biopolymers such as poly(lactic acid) (PLA) and the development of biodegradable materials (Fortunati, Peltzer, et al., 2012; Pei, Zhou, & Berglund, 2010; Petersson, Kvien, & Oksman, 2007).

In our previous studies, we produced a ductile bio-based PLA blend through the addition of 10 wt.% of natural rubber (NR) into the PLA matrix (Bitinis, Verdejo, Cassagnau, & Lopez-Manchado, 2011). Further improvements were obtained by developing PLA/NR/organoclays bionanocomposites, as the organoclays acted as compatibilisers for the immiscible blend (Bitinis, Sanz, et al., 2012; Bitinis, Verdejo, et al., 2012). Nevertheless, it seemed of interest to replace the organoclays by cellulose nanowhiskers in our blend and observe their behavior in an immiscible polymer blend.

Therefore, cellulose nanowhiskers (CNC) were prepared from microcrystalline cellulose and two surface grafting reactions, i.e. long alkyl chain grafting (C18-g-CNC) and PLA chain grafting (PLA-g-CNC), were carried out in order to improve their compatibility with the two components of the blend (Bitinis et al., 2013). The processing conditions were optimized adequately in order to reach a good dispersion of the CNC, combining solvent casting and extrusion and considering the low thermal stability of the filler and their strong aggregation upon drying (Henriksson, Berglund, Isaksson, Lindstrom, & Nishino, 2008; Roman & Winter, 2004). Moreover, the CNC modifications determined their location in the PLA/NR blend and influenced the blend morphology. Thus, CNC and PLA-g-CNC were mainly located in the PLA phase while C18-g-CNC was observed in the NR droplets. The good dispersion of the nanoparticles was demonstrated by TEM images and rheological measurements.

Here, the objective of our work is to relate the morphology of the bionanocomposites to their ultimate properties, which should strongly depend on the location and interactions of the CNC with the two blended polymers. Specially, we report the crystallization, mechanical and biodegradation properties.

* Corresponding author. Tel.: +34 915 622 900; fax: +34 915 644 853.
E-mail address: lmanchado@ictp.csic.es (M.A. López-Manchado).

0144-8617/$ – see front matter © 2013 Elsevier Ltd. All rights reserved.
http://dx.doi.org/10.1016/j.carbpol.2013.03.091

2. Experimental

2.1. Preparation of the nanocomposites

The preparation of the cellulose nanowhiskers, i.e. unmodified cellulose nanocrystal (CNC), cellulose nanocrystal grafted with long alkyl chains (C18-g-CNC) and cellulose nanocrystal grafted with PLA chains (PLA-g-CNC), was described in our previous study (Bitinis et al., 2013). PLA polymer 2002D was provided by NatureWorks® (D-content 4.25%, MI = 5–7 g/10 min, $\rho = 1.24\,g\,cm^{-3}$). Natural rubber (NR) was kindly supplied by Malaysian rubber under the trade name CV60 (Mooney viscosity: ML(1 + 4) 100 °C = 60, $\rho = 0.91\,g\,cm^{-3}$).

NR concentration was fixed at 10 wt.% and the cellulose nanocrystal loading was varied from 1 to 5 wt.%. Samples were prepared by combining solvent casting and extrusion (Bitinis et al., 2013) followed by compression molded (2 min at 10 bars and 170 °C, 2 min at 150 bars and 170 °C, cooled 2 min at 150 bars). The materials resulted in amorphous state.

2.2. Characterizations

2.2.1. Physical properties

Dynamic mechanical analysis was performed on a Mettler Toledo DMA 861^e in tensile mode at 1 Hz as a function of the temperature from −90 °C to 150 °C at a heating rate of 2 °C min^{-1}.

The cold crystallization process was examined in a Mettler Toledo DSC822 differential scanning calorimetry. The following procedure was adopted: samples of about 10 mg were firstly heated from room temperature to 200 °C at a scan rate of 40 °C min^{-1}, maintained at this temperature for 3 min to erase the thermal history, then, were rapidly cooled to 20 °C. Finally, a second heating scan from 20 °C to 200 °C at 2 °C min^{-1} was carried out. The experiments were performed in nitrogen atmosphere.

2.2.2. Mechanical properties

Tensile tests of the samples were measured according to ASTM D 3379-75 specifications on an Instron dynamometer (model 3366) at 23 °C, and at a cross-head speed of 10 mm min^{-1}. At least five specimens of each sample were tested.

2.2.3. Bio-disintegration study

Bio-disintegration study was carried out following the European standard ISO 20200 which considers the disintegration degree of plastic materials under simulated composting conditions in a laboratory-scale test at 58 °C, 50% of humidity and in aerobic conditions. ISO 20200 defines as disintegrable a sample that achieves in 90 days the 90% of disintegration, which means that no more than 10% of the original dry weight has to be retained in a 2 mm sieve. A specific quantity of compost inoculum, supplied by Gesenu S.p.a., was mixed together with the synthetic biowaste prepared with sawdust, rabbit food, starch, sugar, oil and urea as reported in Table 1. The water content of the substrate was around 50 wt.% and the aerobic conditions were guaranteed by periodically mixing it softly.

Table 1
Compost composition.

Components	%
Sawdust	20
Rabbit food	15
Starch	5
Compost inoculum	5
Sugar	2.5
Oil	1.5
Urea	1
Deionized water	50

Compression molded films of 20 mm × 20 mm × 0.30 mm were buried into the organic substrate at 4–6 cm depth in the perforated boxes and incubated at 58 °C. The tested samples were taken out at selected times, washed and dried in an oven at 37 °C for 24 h.

The blends chosen for the disintegrability study were the nanocomposites with 3 wt.% of nanofiller loading. The disintegrability value was obtained normalizing the weight of the samples, at different stages of incubation, with respect to the initial ones. Infrared spectra of the samples were measured in a Jasco FT-IR 615 spectrometer in attenuated total refraction (ATR) mode before and after different times of disintegration in composting conditions.

3. Results and discussion

3.1. Dynamic mechanical analysis

An increase of the mechanical properties and of the storage modulus of PLA/cellulose bionanocomposites have been described by several research groups, although no significant changes were observed regarding PLA tan δ (Lee, Blaker, & Bismarck, 2009; Petersson et al., 2007; Tome et al., 2011). Fig. 1 shows the storage modulus and tan δ of PLA/NR blend and its nanocomposites over a temperature range from −100 to 150 °C.

The E' curve of the blend exhibits two drops corresponding to the glass transition temperature of its constituents. The addition of 3 wt.% of the different types of CNC results in an increase of the modulus value (Fig. 1a). The stronger increases are observed for unmodified CNC and PLA-g-CNC. For C18-g-CNC, the storage modulus difference between the PLA/NR blend and the nanocomposite tends to zero from NR T_g to the PLA T_g and the reinforcing effect decreases with increasing temperature. Moreover, while none of the CNC affects the PLA T_g, a shift of NR T_g toward higher temperature is observed with the addition of C18-g-CNC, increasing from −50.5 °C in the blend to −47.8 °C after the addition of 3 wt.% of C18-g-CNC (Fig. 1b). This shift confirms the affinity of C18-g-CNC to the NR phase that we observed from TEM images (Bitinis et al., 2013), reducing the rubber chain mobility due to the formation of strong nanofiller-rubber interactions. For PLA-g-CNC filled nanocomposites (Fig. 1c), an increase of the storage modulus is observed when increasing the concentration over the entire temperature range while no clear tendency over the polymer T_g is perceived. In fact, the real concentration of C18-g-CNC in the NR phase is higher than the concentration of PLA-g-CNC in the PLA phase, explaining why no changes are observed in the PLA T_g, even if a good affinity is expected between PLA matrix and PLA-g-CNC.

3.2. Crystallization behavior

The cold crystallization behavior of the PLA/NR/CNC nanocomposites was studied by DSC dynamic measurements, as pictured in Fig. 2 and reported in Table 2. No changes of the PLA T_g are observed with the addition of the cellulose nanowhiskers. As already reported, NR acts as a nucleating agent for the PLA matrix, resulting in a decrease of the PLA T_c in the polymer blend (Bitinis et al., 2011). DSC thermograms show the presence of two melting peaks during the melting process. This crystallization behavior of PLA has been ascribed to either a re-crystallization process, i.e. the change of small and imperfect crystals into more stable crystals through melting and recrystallisation at low heating rates (Yasuniwa, Tsubakihara, Sugimoto, & Nakafuku, 2004), or the presence of two crystalline phases (Eling, Gogolewski, & Pennings, 1982).

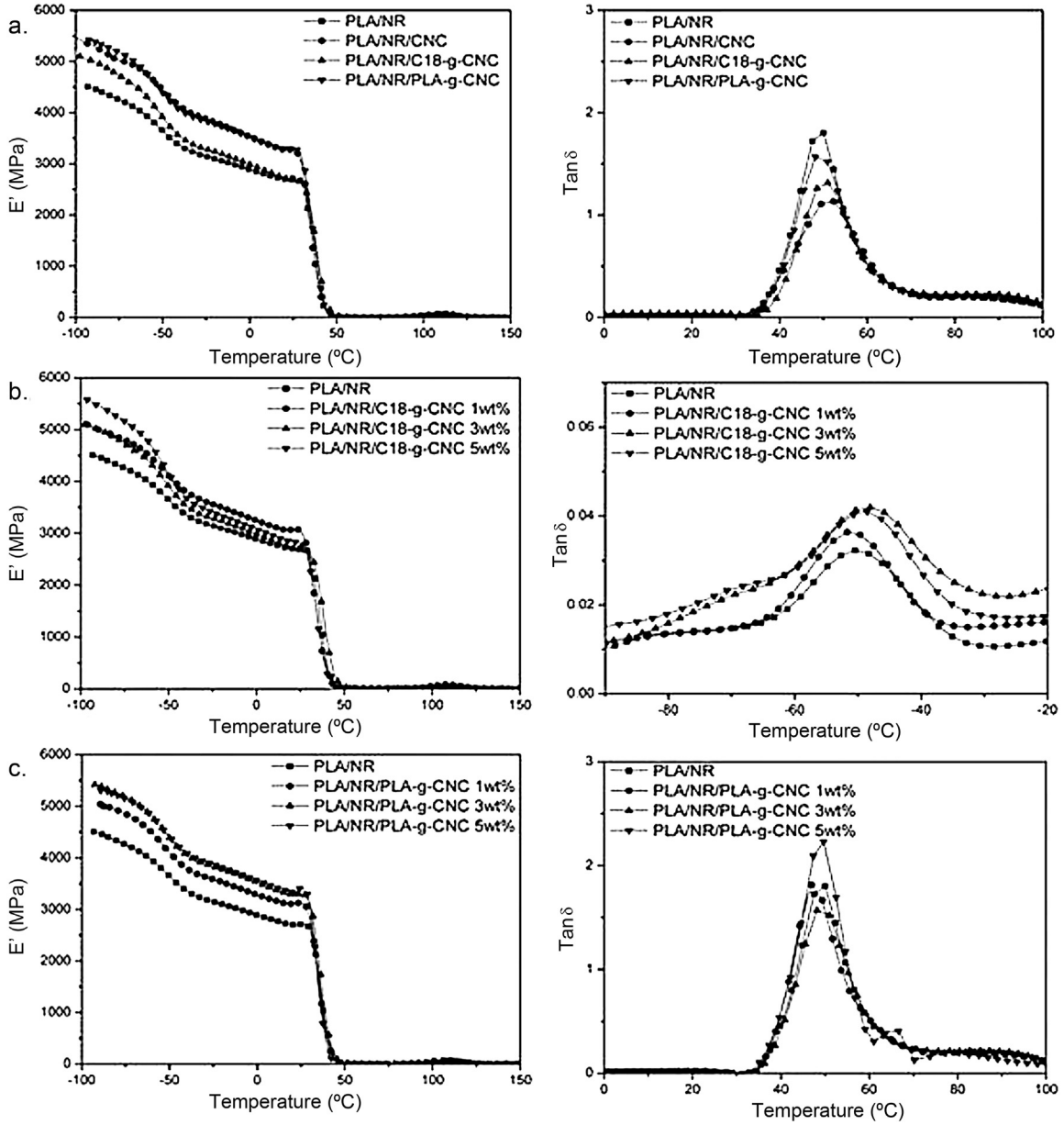

Fig. 1. Temperature dependence of (a) E' and tan δ (referred to PLA T_g) of PLA-NR blend and its nanocomposites with cellulose nanowhisker type at 3 wt.%, (b) E' and tan δ (referred to the T_g of NR) of PLA-NR blend and its nanocomposites with C18-g-CNC concentration and (c) E' and tan δ (referred to PLA T_g) of PLA-NR blend and its nanocomposites with PLA-g-CNC concentration.

Fig. 2 displays the influence of different cellulose nanowhiskers over the crystallization behavior of the PLA/NR blend. An opposite effect is observed depending on the whisker modifications. The addition of 3 wt.% of unmodified CNC and C18-g-CNC induces an increase of PLA T_c while a slight decrease is reported for PLA-g-CNC. As observed in Table 2, this effect is more evident as the nanowhisker concentration increases in the composite. The incorporation of CNC has no apparent effect on the PLA melting peaks.

Table 2
DSC data of PLA/NR/CNC nanocomposites (second heating scan).

	T_c (°C)	ΔH_c (J g^{-1})	T_{m1} (°C)	T_{m2} (°C)	ΔH_{mtot} (J g^{-1})
PLA	113.8	−27.3	146.9	152.5	23.4
PLA/NR	104.9	−22.2	145.2	152.3	21.8
PLA/NR/CNC 3 wt.%	106.0	−22.8	145.7	152.6	23.0
PLA/NR/C18-g-CNC 1 wt.%	107.1	−22.7	145.6	152.5	21.8
PLA/NR/C18-g-CNC 3 wt.%	110.0	−23.9	146.8	153.0	20.8
PLA/NR/C18-g-CNC 5 wt.%	111.5	−23.7	147.0	153.2	22.5
PLA/NR/PLA-g-CNC 1 wt.%	103.7	−22.3	144.9	152.5	20.5
PLA/NR/PLA-g-CNC 3 wt.%	103.0	−21.5	145.6	153.6	21.2
PLA/NR/PLA-g-CNC 5 wt.%	100.9	−24.1	145.6	153.9	23.8

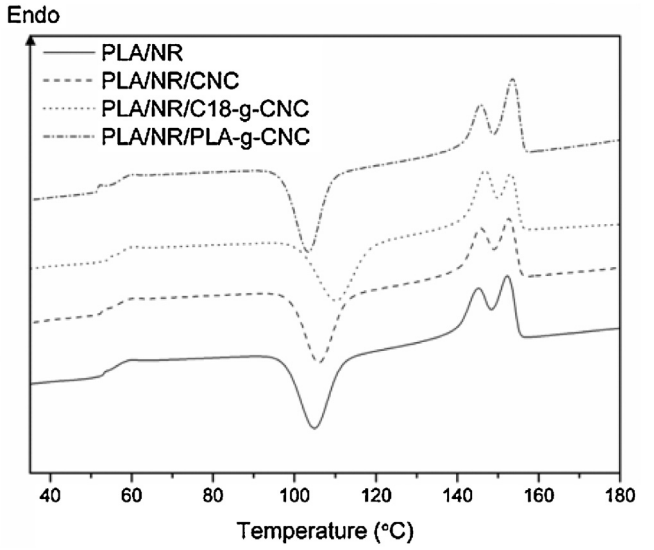

Fig. 2. Dynamic crystallization of PLA/NR/CNC bionanocomposites at 3 wt.% of CNC as a function of the type of modification.

Both location and affinity of the bioparticles with the two polymers play an important role on the crystallinity behavior of the nanocomposites. Unmodified CNC and PLA-g-CNC are both located in the PLA phase. However, while the presence of CNC appears to affect negatively the PLA crystallization, PLA-g-CNC shows a nucleating effect over the PLA/NR blend. This different behavior can be attributed to the better compatibility of PLA-g-CNC with the PLA matrix. The nucleating effect of PLA-g-CNC has been reported by Goffin et al. (2011). Nevertheless, they also observed a strong decrease of the PLA T_g due to the presence of short PLA-grafted or non-grafted chains that could act as plasticizers. Therefore, it was difficult to conclude which effect was more predominant between the nucleation induced by PLA-g-CNC or the plasticization effect of PLA short chains. In the current study, no changes on the PLA T_g were observed by neither DMA nor DSC measurements. Thus, the nucleating effect of well dispersed and modified CNC is predominant.

On the other hand, the addition of C18-g-CNC leads to an increase of PLA cold crystallization temperature (Table 2). From DMA measurements and TEM images, it was demonstrated that C18-g-CNC affinity toward NR was higher than toward PLA. In this case, the nucleating effect of the NR droplets could be reduced due to the interaction of C18-g-CNC with NR.

3.3. Mechanical properties

As already reported, the addition of a 10 wt.% of NR to the PLA matrix leads to a strong increase of the elongation at break (Bitinis et al., 2011) (Table 3). Retaining the ductile behavior of the PLA/NR blend after the addition of nanofillers was a desired result. Therefore, the study of the mechanical properties of cellulose nanowhisker based nanocomposites is critical in the development of these systems.

No real improvements of Young's modulus or tensile strength are observed with the addition of unmodified CNC. The average elongation of this material is not reported in Table 3 because of the large deviations of the results, which vary between 8% and 148%. TEM images demonstrated that unmodified CNC are preferentially located in the PLA phase. A good dispersion of the fillers was observed by TEM images and rheological measurements (Bitinis et al., 2013), nevertheless a lack of compatibility between unmodified CNC and PLA matrix could be responsible for the inhomogeneous values of the elongation at break.

The addition of C18-g-CNC leads to a progressive decrease of the Young's modulus and the tensile strength with increasing concentration of whiskers. The elongation at break remains over 150% for concentrations of 1 wt.% and 3 wt.% while decreases to about a third of that value for 5 wt.%. These mechanical properties are similar to those obtained for C15A montmorillonites and are attributed to the affinity of the C18-g-CNC toward the NR phase (Bitinis, Verdejo, et al., 2012). Furthermore, the short grafted chains may act as plasticizer influencing the T_g of the nanocomposite system (Greco, Gennaro, & Rizzo, 2012).

Interesting results are obtained with the addition of PLA-g-CNC. The tensile strength is maintained with increasing the concentration of nanocrystals while the Young's modulus slightly increases. The elongation at break is also maintained for concentrations of 1 wt.% and 3 wt.%, while more heterogeneous results are observed at 5 wt.%. The presence of PLA grafted short chains on the CNC surface appears to be an effective compatibilizer between CNC and PLA to maintain the ductile property of the PLA/NR blend, even though the PLA-g-CNC are preferentially located in the PLA phase. Moreover, small PLA chains could also help to improve PLA matrix flexibility even if no changes in PLA T_g were observed.

3.4. Disintegration in composting conditions

The biodegradation of PLA in compost is one of its most attractive properties for packaging applications (Kale, Auras, Singh, & Narayan, 2007). Its degradation usually starts with the hydrolysis of the PLA chains induced by the diffusion of water into the materials. The PLA molecular weight reduction caused by the random non-enzymatic chain scissions of the ester groups leads to the formation of oligomers and lactic acid. When the molecular weight reaches about 10,000–20,000 g mol^{-1}, microorganisms such as fungi and bacteria can metabolized the macromolecules converting them to carbon dioxide, water and hummus, this step occurring at the surface of the material (Fukushima, Abbate, Tabuani, Gennari, & Camino, 2009; Kale et al., 2007; Paul et al., 2005).

The effect of nanoparticles addition over PLA biodegradation in compost has been reported over the past few years; especially for layered silicates, leading to opposite conclusions (Fukushima et al., 2009; Ray, Yamada, Okamoto, & Ueda, 2003). The influence of nanoparticles over the degradation process strongly depends on their hydrophilicity and their dispersion (Fukushima et al., 2009; Lee et al., 2002; Ray et al., 2003). The improved barrier properties of the nanocomposites could also have a negative effect over the water diffusion through the bulk, retarding the biodegradability (Lee et al., 2002).

Nevertheless, no reports were found on the influence of bionanoparticles over PLA biodegradation. The biodegradation in compost of PLA composites reinforced with microcrystalline cellulose, wood flour and wood pulp was described by Mathew, Oksman, and Sain (2005). Surprisingly, a slower disintegration rate was observed for the composites and was attributed to a higher resistance to water uptake and diffusion through the composites compared to pure PLA.

Here, the study of the disintegration of PLA/NR/cellulose nanowhisker materials was carried out for 3 wt.% of nanofillers. Additionally, PLA and PLA/NR blend were also studied for comparison. As the crystallinity of the materials can strongly influences its degradation rate, all samples were prepared to be amorphous (Iannace, Maffezzoli, Leo, & Nicolais, 2001).

Fig. 3 shows the samples taken out at different times of composting. During the first week, whitening and deformation of the surface are detected for all materials. These observations are a signal that the hydrolytic degradation has started. The opacity observed is

Table 3
Mechanical properties of PLA/NR/CNC nanocomposites.

	Young's modulus (MPa)	Tensile strength (MPa)	Elongation at break (%)
PLA	2553 ± 68	60.4 ± 1.5	4 ± 1
PLA/NR	2045 ± 86	41.1 ± 0.9	166 ± 22
PLA/NR/CNC 3 wt.%	2043 ± 142	42.4 ± 1.1	From 8 to 148
PLA/NR/C18-g-CNC 1 wt.%	2260 ± 138	39.9 ± 1.3	178 ± 6
PLA/NR/C18-g-CNC 3 wt.%	1876 ± 111	33.9 ± 0.9	152 ± 12
PLA/NR/C18-g-CNC 5 wt.%	1785 ± 77	31.1 ± 0.6	53 ± 13
PLA/NR/PLA-g-CNC 1 wt.%	1892 ± 58	42.0 ± 1.0	163 ± 8
PLA/NR/PLA-g-CNC 3 wt.%	1986 ± 88	41.1 ± 0.8	167 ± 20
PLA/NR/PLA-g-CNC 5 wt.%	2047 ± 135	41.4 ± 2.1	From 58 to 191

due to changes of the refractive index which can be attributed to the water absorption and to the low molecular weight compounds formed by the hydrolytic degradation (Fukushima, Tabuani, Abbate, Arena, & Ferreri, 2010). Moreover, the formation of holes in the materials or an increase of crystallinity during degradation can also be responsible for the opacity (Paul et al., 2005). It should be taken into account that the degradation experiments took place at 58 °C, which is closed to the T_g of the matrix. This could increase the chains mobility, inducing the crystallization of the PLA matrix. At the 10th day, fragmentation and weight loss of the samples are already observed for all the materials except C18-g-CNC nanocomposite, which starts to fragment after the 15th day.

Fig. 4 reports the evolution of the material disintegrability with the composting time. It can be observed that after 31 days of composting, all materials reach a 100% of disintegration. A slight delay of PLA/NR blend disintegration is observed when compared to PLA. It has been demonstrated that natural rubber undergoes microbial degradation and possible biodegradation involving oxidative cleavage of the double bond of the polymer backbone (Bode, Kerkhoff, & Jendrossek, 2001; Rose & Steinbuchel, 2005). However, the rubber biodegradation is a slow process and this explains the observed results for the blend when compared to PLA.

The addition of the unmodified CNC does not affect the disintegration rate of the blend. Although the addition of a hydrophilic filler is expected to accelerate the degradation rate of the PLA/NR material, CNC could also inhibit water diffusion, explaining the obtained results (Fortunati, Peltzer, et al., 2012; Mathew et al., 2005). Here, the two effects appear to counterbalance each other. Meanwhile, the modified cellulose nanowhiskers delay the disintegration rate, the slowest rate being observed for C18-g-CNC. The modification reaction of cellulose whiskers increases the hydrophobicity of the nanofillers, especially for C18-g-CNC, which could then hinder hydrolytic degradation.

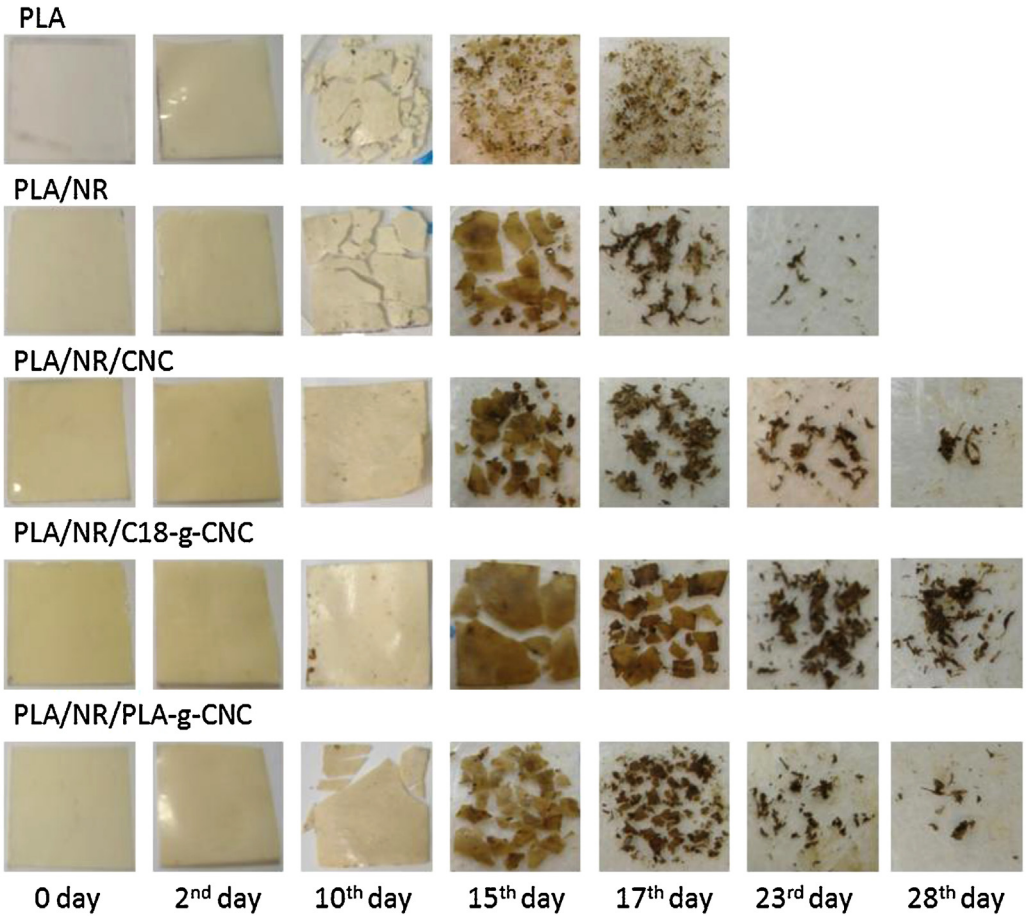

Fig. 3. Disintegration of the materials at different times of composting.

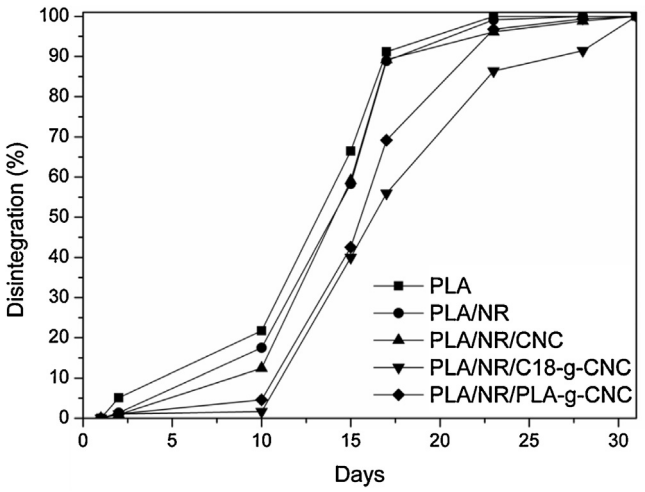

Fig. 4. Evolution of disintegration of the materials with composting time.

Fig. 5 shows the FT-IR spectra of PLA/NR and PLA/NR/C18-g-CNC at different incubation times. Both materials present at the beginning of the experiment the typical sharp band at 1750 cm^{-1} of the carbonyl group stretching (—C=O) and the —C—O— stretching band of the —CH—O— group at 1182 cm^{-1} of PLA. Observing the PLA spectra evolution, a new band appears at 1600 cm^{-1} corresponding to the carboxylate ion, while the band at 1260 cm^{-1} corresponding to the —C—O— stretching disappears (15 days). These observations have previously been reported and are due to the depletion of the lactic acid and oligomers by the microorganism leaving a carboxylate ion at the end of the chain (Fortunati, Armentano, et al., 2012; Khabbaz, Karlsson, & Albertsson, 2000). Moreover, after 17 days of incubation, the characteristic bands of PLA spectra disappeared. On another hand, a new band progressively appears at 830 cm^{-1} (cis-1,4-double bond), due to the increasing concentration of NR in the blend as PLA degrades. The process of degradation is slower for C18-g-CNC composites than for PLA/NR blend.

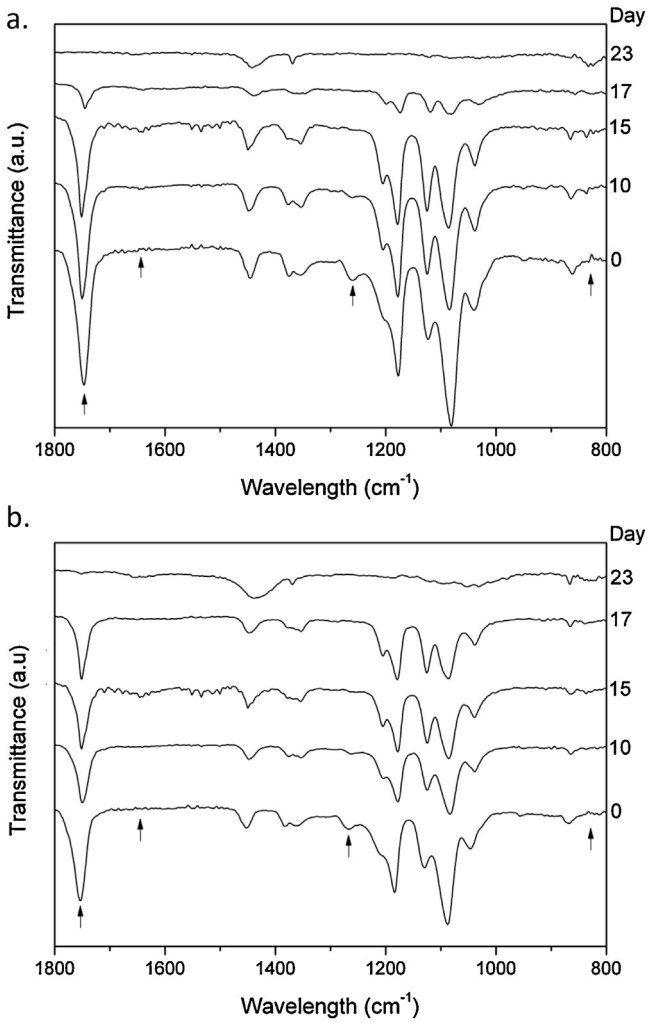

Fig. 5. FT-IR spectra of (a) PLA/NR and (b) PLA/NR/C18-g-CNC as function of the disintegration time.

4. Conclusions

The properties of new PLA/NR/CNC bionanocomposites based on unmodified cellulose nanowhiskers, alkyl chain grafted CNC (C18-g-CNC) and PLA grafted CNC (PLA-g-CNC) were described. The nanocomposites showed different morphologies which strongly influenced their ultimate properties. CNC and PLA-g-CNC displayed a higher affinity to the PLA phase while C18-g-CNC exhibited strong interactions with the rubbery phase. Moreover, PLA-g-CNC presented an interesting nucleating effect over the PLA matrix, while, on the contrary, C18-g-PLA inhibited the nucleating effect of the NR droplets. Interestingly, a high elongation under tensile conditions was maintained for the bionanocomposites. Furthermore, all materials reached a 100% of disintegration in composting conditions, even if the introduction of hydrophobic nanofillers delayed the process.

Acknowledgments

NB thanks the CSIC for a JAE-Pre grant. EF gratefully acknowledges the financial support from the National Consortium of Materials Science and Technology (INSTM). The Authors acknowledge Gesenu S.p.a. for compost supply.

References

Azizi Samir, M. A. S., Alloin, F., & Dufresne, A. (2005). Review of recent research into cellulosic whiskers, their properties and their application in nanocomposite field. *Biomacromolecules*, *6*(2), 612–626.

Bitinis, N., Sanz, A., Nogales, A., Verdejo, R., Lopez-Manchado, M. A., & Ezquerra, T. A. (2012). Deformation mechanisms in polylactic acid/natural rubber/organoclay bionanocomposites as revealed by synchrotron X-ray scattering. *Soft Matter*, *8*(34), 8990–8997.

Bitinis, N., Verdejo, R., Bras, J., Fortunati, E., Torre, L., & López-Manchado, M. A. (2013). Poly(lactic acid)/natural rubber/cellulose nanocrystal bionanocomposites Part I. Processing and morphology. *Carbohydrate Polymers*, http://dx.doi.org/10.1016/j.carbpol.2013.02.068

Bitinis, N., Verdejo, R., Cassagnau, P., & Lopez-Manchado, M. (2011). Structure and properties of polylactide/natural rubber blends. *Materials Chemistry and Physics*, *129*(3), 823–831.

Bitinis, N., Verdejo, R., Maya, E. M., Espuche, E., Cassagnau, P., & Lopez-Manchado, M. A. (2012). Physicochemical properties of organoclay filled polylactic acid/natural rubber blend bionanocomposites. *Composites Science and Technology*, *72*(2), 305–313.

Bode, H. B., Kerkhoff, K., & Jendrossek, D. (2001). Bacterial degradation of natural and synthetic rubber. *Biomacromolecules*, *2*(1), 295–303.

Eling, B., Gogolewski, S., & Pennings, A. J. (1982). Biodegradable materials of poly(L-lactic acid): 1. Melt-spun and solution-spun fibres. *Polymer*, *23*(11), 1587–1593.

Fortunati, E., Armentano, I., Iannoni, A., Barbale, M., Zaccheo, S., Scavone, M., et al. (2012). New multifunctional poly(lactide acid) composites: Mechanical, antibacterial, and degradation properties. *Journal of Applied Polymer Science*, *124*(1), 87–98.

Fortunati, E., Peltzer, M., Armentano, I., Torre, L., Jimenez, A., & Kenny, J. M. (2012). Effects of modified cellulose nanocrystals on the barrier and migration properties of PLA nano-biocomposites. *Carbohydrate Polymers*, *90*(2), 948–956.

Fukushima, K., Abbate, C., Tabuani, D., Gennari, M., & Camino, G. (2009). Biodegradation of poly(lactic acid) and its nanocomposites. *Polymer Degradation and Stability*, *94*(10), 1646–1655.

Fukushima, K., Tabuani, D., Abbate, C., Arena, M., & Ferreri, L. (2010). Effect of sepiolite on the biodegradation of poly(lactic acid) and polycaprolactone. *Polymer Degradation and Stability*, *95*(10), 2049–2056.

Greco, A., Gennaro, R., & Rizzo, M. (2012). Glass transition and cooperative rearranging regions in amorphous thermoplastic nanocomposites. *Polymer International*, *61*(8), 1326–1333.

Goffin, A.-L., Raquez, J.-M., Duquesne, E., Siqueira, G., Habibi, Y., Dufresne, A., et al. (2011). From interfacial ring-opening polymerization to melt processing of cellulose nanowhisker-filled polylactide-based nanocomposites. *Biomacromolecules*, *12*(7), 2456–2465.

Habibi, Y., Lucia, L. A., & Rojas, O. J. (2010). Cellulose nanocrystals: Chemistry, self-assembly, and applications. *Chemical Reviews*, *110*(6), 3479–3500.

Henriksson, M., Berglund, L. A., Isaksson, P., Lindstrom, T., & Nishino, T. (2008). Cellulose nanopaper structures of high toughness. *Biomacromolecules*, *9*(6), 1579–1585.

Iannace, S., Maffezzoli, A., Leo, G., & Nicolais, L. (2001). Influence of the crystal and amorphous phase morphology on hydrolytic degradation of PLLA subjected to different processing conditions. *Polymer*, *42*(8), 3799–3807.

Kale, G., Auras, R., Singh, S. P., & Narayan, R. (2007). Biodegradability of polylactide bottles in real and simulated composting conditions. *Polymer Testing*, *26*(8), 1049–1061.

Kale, G., Kijchavengkul, T., Auras, R., Rubino, M., Selke, S. E., & Singh, S. P. (2007). Compostability of bioplastic packaging materials: An overview. *Macromolecular Bioscience*, *7*(3), 255–277.

Khabbaz, F., Karlsson, S., & Albertsson, A. C. (2000). Py-GC/MS an effective technique to characterizing of degradation mechanism of poly(L-lactide) in the different environment. *Journal of Applied Polymer Science*, *78*(13), 2369–2378.

Lee, K. Y., Blaker, J. J., & Bismarck, A. (2009). Surface functionalisation of bacterial cellulose as the route to produce green polylactide nanocomposites with improved properties. *Composites Science and Technology*, *69*(15–16), 2724–2733.

Lee, S. R., Park, H. M., Lim, H., Kang, T. Y., Li, X. C., Cho, W. J., et al. (2002). Microstructure, tensile properties, and biodegradability of aliphatic polyester/clay nanocomposites. *Polymer*, *43*(8), 2495–2500.

Mathew, A. P., Oksman, K., & Sain, M. (2005). Mechanical properties of biodegradable composites from poly lactic acid (PLA) and microcrystalline cellulose (MCC). *Journal of Applied Polymer Science*, *97*(5), 2014–2025.

Paul, M. A., Delcourt, C., Alexandre, M., Degee, P., Monteverde, F., & Dubois, P. (2005). Polylactide/montmorillonite nanocomposites: Study of the hydrolytic degradation. *Polymer Degradation and Stability*, *87*(3), 535–542.

Pei, A. H., Zhou, Q., & Berglund, L. A. (2010). Functionalized cellulose nanocrystals as biobased nucleation agents in poly(L-lactide) (PLLA) – Crystallization and mechanical property effects. *Composites Science and Technology*, *70*(5), 815–821.

Petersson, L., Kvien, I., & Oksman, K. (2007). Structure and thermal properties of poly(lactic acid)/cellulose whiskers nanocomposite materials. *Composites Science and Technology*, *67*(11–12), 2535–2544.

Ray, S. S., Yamada, K., Okamoto, M., & Ueda, K. (2003). Control of biodegradability of polylactide via nanocomposite technology. *Macromolecular Materials and Engineering*, *288*(3), 203–208.

Roman, M., & Winter, W. T. (2004). Effect of sulfate groups from sulfuric acid hydrolysis on the thermal degradation behavior of bacterial cellulose. *Biomacromolecules*, *5*(5), 1671–1677.

Rose, K., & Steinbuchel, A. (2005). Biodegradation of natural rubber and related compounds: Recent insights into a hardly understood catabolic capability of microorganisms. *Applied and Environmental Microbiology*, *71*(6), 2803–2812.

Tome, L. C., Pinto, R. J B., Trovatti, E., Freire, C. S. R., Silvestre, A. J. D., Neto, C. P., et al. (2011). Transparent bionanocomposites with improved properties prepared from acetylated bacterial cellulose and poly(lactic acid) through a simple approach. *Green Chemistry*, *13*(2), 419–427.

Yasuniwa, M., Tsubakihara, S., Sugimoto, Y., & Nakafuku, C. (2004). Thermal analysis of the double-melting behavior of poly(L-lactic acid). *Journal of Polymer Science Part B: Polymer Physics*, *42*(1), 25–32.